ATMOSPHERIC MOTION VECTOR RETRIEVAL USING THE TOTAL VARIATION-BASED OPTICAL FLOW METHOD

Igor Yanovsky[1], *Derek Posselt*[1], *Longtao Wu*[1], *Svetla Hristova-Veleva*[1], *Hai Nguyen*[1], *Bjorn Lambrigtsen*[1] *and Xubin Zeng*[2]

[1]Jet Propulsion Laboratory, California Institute of Technology, Pasadena, CA, USA
[2]Department of Hydrology and Atmospheric Sciences, University of Arizona, Tucson, AZ, USA

ABSTRACT

Atmospheric motion vector (AMV) retrieval from water vapor measurements is important in climate research and weather forecasting. However, conventional feature tracking methods for AMV retrievals generate velocity fields with gaps and large errors. In this work, we test the optical flow algorithm by generating a nature run of a convective weather phenomenon, which provides water vapor variables and wind vector fields at various pressure levels. We show that our optical flow algorithm generates superior performance when compared with traditional feature tracking algorithms used in operational centers, generating dense AMVs with no gaps and significantly improving AMV accuracy. The optical flow algorithm performs well down to very low wind speeds and does not require a low-wind cutoff threshold. In our studies, we considered various measurement configurations, including water vapor retrievals at different temporal resolutions and found that the optical flow algorithm is not sensitive to the time interval between images.

Index Terms— Atmospheric motion vector retrieval, feature tracking, optical flow, total variation, water vapor

1. INTRODUCTION

Knowledge of atmospheric motion vectors (AMVs) is important for climate studies and weather prediction. AMVs are key to understanding of the changing aspects of convective storms and extreme weather phenomena. AMV estimates are already routinely produced from the current global satellite constellation. AMVs are derived by tracking features in sequences of geostationary (GEO) or high latitude low Earth orbit (LEO) images spaced at regular intervals in time. However, AMV estimation from radiances captured by satellite passive infrared or microwave instruments is a challenging problem. Current AMV retrieval methods often produce vector fields with significant errors. In particular, in [1], the authors used a traditional feature tracking method for AMV retrieval. However, such methods do not capture displacement fields in subpixel resolution. They also result in an over-smoothed displacement fields.

This research was carried out in part at the Jet Propulsion Laboratory, California Institute of Technology, under a contract with the National Aeronautics and Space Administration.

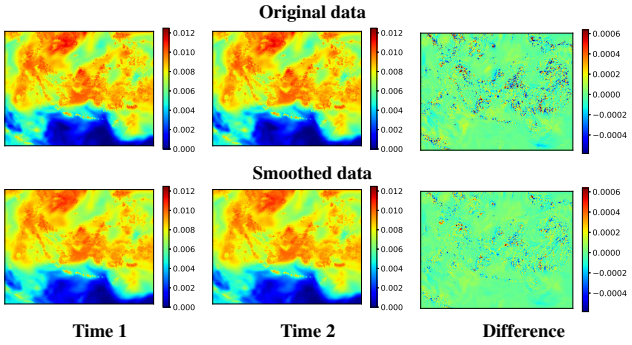

Fig. 1. Original and smoothed water vapor images (in units of kg/kg) that are 576 seconds apart at 700 hPa pressure level are shown.

Non-variational physical based image registration methods have been shown to be successful for retrieving displacement fields in atmospheric and oceanic data [2, 3], but not in capturing AMVs using water vapor data. In this work, our goal is to retrieve AMVs from an image sequence of water vapor measurements using the efficient and robust variational optical flow algorithm. The optical flow algorithm [4, 5, 6] we propose to use minimizes the L1 norm of image intensity differences [7, 8], enforcing the conservation of pixel brightness across a pair of images, and has total variation regularization constraint [9] on displacement fields. In order to assess the results generated by the optical flow algorithm, we employ a high-resolution numerical weather prediction model [10] to generate a nature run of a convective weather scene, which provides water vapor quantities and nature run wind velocity field at different pressure levels. We then use the optical flow algorithm to derive the AMVs from a sequence of water vapor quantities and compare them to the nature run wind velocities, thus estimating AMV retrieval errors. We show that the optical flow algorithm generates dense AMVs for every pixel in a pair of images, with higher spatial and temporal resolution, and with smaller errors compared to the feature match-

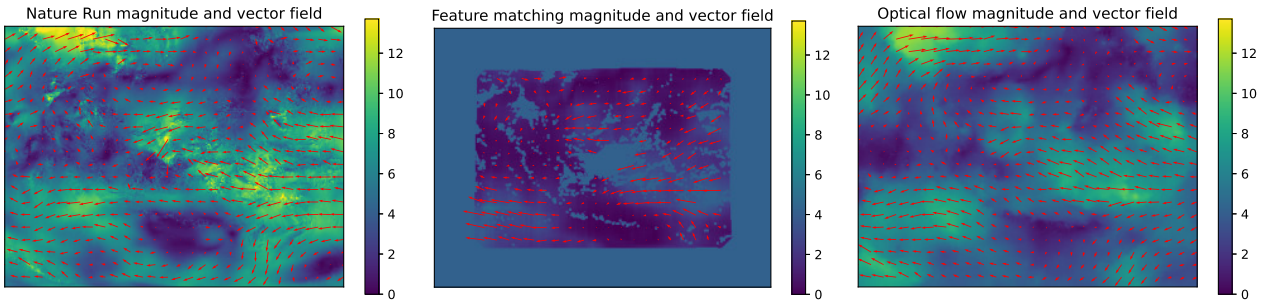

Fig. 2. Wind speed (in units of m/s) and wind vector fields for nature run (left), feature matching result (middle), and optical flow result (right) for smoothed 700 hPa water vapor data 576 seconds apart.

ing method. Our work is critical for determining the mission architecture and projected instrument performance for future satellite missions designed to retrieve atmospheric winds.

2. THE FEATURE MATCHING METHOD

Local area feature matching is a common technique to track atmospheric features in sequential imagery [1]. The feature matching algorithm finds local gradients in the first image that match gradients in the second image. These features are tracked forward in subsequent images. The algorithm determines a search area containing a range of possible target coordinate matches for each source coordinate and then computes a cost function, which is a normalized sum of absolute differences over a specified window patch. The minimum of the cost function represents the best match in this search area. The feature matching is typically applied to three sequential images, including the image in the center in time. The algorithm considers every possible tracking window over the entire spatial image domain. For each valid estimate, the vector magnitude of difference is determined, and if it is less than a specified threshold, the average over the patch is considered as the retrieved velocity vector. The algorithm is not guaranteed to find a match of all grid points. Also, the vector field obtained using the algorithm is usually oversmoothed.

3. THE TV-L1 OPTICAL FLOW METHOD

Given the image I_1 at time t_1 and image I_2 at $t_2 > t_1$, we seek to find the displacement field $u = (u_1, u_2)$ that transforms I_1 into correspondence with I_2. We say that the deformed I_1 image aligns with I_2 if deformed I_1 is close to I_2 in some norm. The optical flow brightness constancy assumption is that the pixel intensities remain constant along the trajectories of the moving particles:

$$I_1(x+u) - I_2(x) = 0. \tag{1}$$

The TV-L1 optical flow algorithm [4, 5, 6] we propose to use minimizes the L1 norm of image intensity differences and has total variation regularization on displacement fields:

$$E(u) = \lambda \int_\Omega |I_1(x+u) - I_2(x)|\, dx \tag{2}$$

$$+ \int_\Omega \sqrt{|\nabla u_1|^2 + |\nabla u_2|^2}\, dx. \tag{3}$$

The first term, which is the fidelity term, is the optical flow constraint. The second term, which is the regularization term, allows the optical flow algorithm to preserve discontinuities in the wind field. The optical flow algorithm is robust to noise and generates dense AMV fields, with wind vectors calculated at every pixel.

4. RESULTS AND DISCUSSION

In our experiments, we considered a simulated water vapor dataset capturing tropical convection over the Maritime continent on July 10, 2008. The nature run data was originally simulated at 3.5 km resolution, and subsampled at every 3 points to arrive at what we call the original dataset. In order to construct the smoothed dataset, we first applied vertical smoothing to the nature run data [11]. We then blurred the data with the truncated Gaussian kernel with standard deviation equal to 6.85 km horizontally in order to model the characteristics of passive infrared or microwave remote sensing, and subsequently subsampled the data at every 3 points. Both original and smoothed datasets consist of 433 by 333 pixel images of 10.5 km spatial resolution and 72 seconds temporal resolution. The datasets are defined at four different pressure levels (850, 700, 500, 300 hPa).

Pairs of images (as well as their differences) for both original and smoothed datasets that are 576 seconds apart and at 700 hPa pressure level are shown in Figure 1. We tested the total variation-based optical flow algorithm discussed in this paper as well as the feature matching algorithm of [1] on both the original and smoothed water vapor data. We compared the computed velocity fields using the feature matching and the optical flow algorithms to the nature run (ground truth) wind vectors.

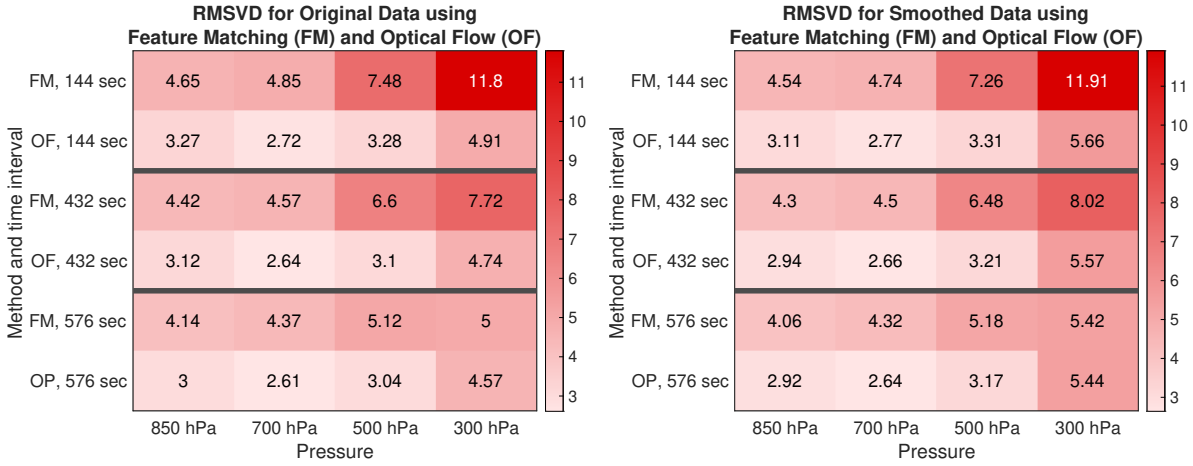

Fig. 3. RMSVD errors (in units of m/s) obtained with feature matching (FM) and optical flow (OF) methods on original data (left figure) and smoothed data (right figure) at different time intervals and at different pressure levels. Compared to the feature matching algorithm, the optical flow algorithm improves AMV accuracy by 42% on original data and 39% on smoothed data on average.

Figure 2 shows nature run wind speeds and wind vectors as well as AMVs obtained using the feature matching and the optical flow algorithms. In this experiment, we considered smoothed water vapor data, at 576 seconds apart, and at 700 hPa pressure level. Note that the feature matching algorithm cannot compute AMVs near the boundaries or where the data is masked due to heavy precipitation (>1 mm/hr) and doesn't compute AMVs at very low (e.g., 1-5 m/s) wind speeds. The total variation-based optical flow algorithm, on the other hand, fills in masked regions using bicubic interpolation before the optical flow is performed. We can observe that the optical flow wind speeds and wind field more closely represent the nature run wind field, with the feature matching speed map being smooth and with less contrast.

Figure 3 shows root mean square vector difference (RMSVD) errors obtained with feature matching and optical flow methods on original data and smoothed data at 144, 432, and 576 second time intervals and at 850, 700, 500, and 300 hPa pressure levels. Compared to the feature matching algorithm, the optical flow algorithm improves AMV accuracy by 42% on original data and 39% on smoothed data on average.

Figure 4(left) shows nature run wind magnitude, RMSVD of mean nature run vector field, as well as RMSVD of feature matching and optical flow results (averaged over all time intervals) versus pressure level on original and smoothed data. We observe that errors are proportional to the wind speed (see the Nature Run magnitude plot). We should note that the nature run wind magnitude is a point of reference – this plot shows the error of an identically zero wind retrieval. That is, the nature run magnitude can be interpreted as the difference between the nature run vector field and the zero wind vector field. If RMSVD from the retrieval is greater than the actual standard deviation of the wind, the retrieval does not have any values; if the former is close to the latter, the retrieval still does not have much information. A more rigorous default estimate is to consider the mean nature run vector field and how it compares with the true nature field. Again, if RMSVD from the retrieval is greater than the RMSVD of the mean nature run vector field, the retrieval does not have any values; if the former is close to the latter, the retrieval still does not have much information. We observe that the plot of RMSVD for optical flow retrieval is considerably below the plot of RMSVD for mean vector field, which means that the optical flow retrieval carries a lot of information.

Figure 4(right) shows nature run wind magnitude, RMSVD of mean nature run vector field, as well as RMSVD of feature matching and optical flow results (averaged over all pressure levels) versus time interval on original and smoothed data. We observe that feature matching has a strong dependence on time interval. However, there is no significant dependence on time interval for the optical flow results – an important point allowing more flexibility when designing future missions.

5. ACKNOWLEDGMENT

The authors would like to thank Hui Su for helpful discussions.

6. REFERENCES

[1] Derek J. Posselt, Longtao Wu, Kevin Mueller, Lei Huang, Fredrick W. Irion, Shannon Brown, Hui Su, David Santek, and Christopher S. Velden, "Quantitative assessment of state-dependent atmospheric motion vector uncertainties," *Journal of Applied Meteorology and Climatology*, vol. 58, no. 11, pp. 2479 – 2495, 2019.

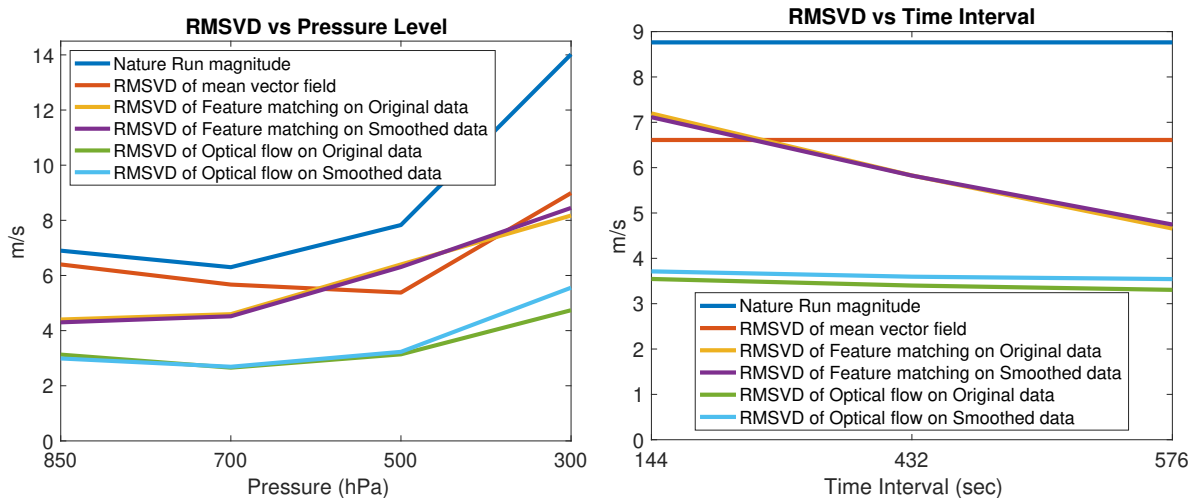

Fig. 4. Left figure shows nature run wind magnitude (in units of m/s), RMSVD of mean nature run vector field, as well as RMSVD of feature matching and optical flow results (averaged over all time intervals) versus pressure level on original and smoothed data. We observe that errors are proportional to the wind speed (see the Nature Run magnitude plot). We also observe that the optical flow retrieval carries a lot of information. Right figure shows nature run wind magnitude, RMSVD of mean nature run vector field, as well as RMSVD of feature matching and optical flow results (averaged over all pressure levels) versus time interval on original and smoothed data. We observe that feature matching has a strong dependence on time interval. There is no significant dependence on time interval for optical flow.

[2] I. Yanovsky and B. Lambrigtsen, "Enhancing the temporal resolution of image sequences capturing evolving weather phenomena," *Remote Sensing Letters*, vol. 7, no. 3, pp. 239–248, 2016.

[3] Igor Yanovsky, Benjamin Holt, and Francois Ayoub, "Deriving velocity fields of submesoscale eddies using multi-sensor imagery," in *IGARSS 2020 - 2020 IEEE International Geoscience and Remote Sensing Symposium*, 2020, pp. 1921–1924.

[4] C. Zach, T. Pock, and H. Bischof, "A duality based approach for realtime TV-L1 optical flow," in *Pattern Recognition*, Fred A. Hamprecht, Christoph Schnörr, and Bernd Jähne, Eds., Berlin, Heidelberg, 2007, pp. 214–223, Springer Berlin Heidelberg.

[5] Andreas Wedel, Thomas Pock, Christopher Zach, Horst Bischof, and Daniel Cremers, "An improved algorithm for TV-L1 optical flow," in *Statistical and Geometrical Approaches to Visual Motion Analysis*, Daniel Cremers, Bodo Rosenhahn, Alan L. Yuille, and Frank R. Schmidt, Eds., Berlin, Heidelberg, 2009, pp. 23–45, Springer Berlin Heidelberg.

[6] Stéfan van der Walt, Johannes L. Schönberger, Juan Nunez-Iglesias, François Boulogne, Joshua D. Warner, Neil Yager, Emmanuelle Gouillart, Tony Yu, and the scikit-image contributors, "scikit-image: image processing in Python," *PeerJ*, vol. 2, pp. e453, June 2014.

[7] S. Alliney, "Digital filters as absolute norm regularizers," *IEEE Transactions on Signal Processing*, vol. 40, no. 6, pp. 1548–1562, 1992.

[8] Y. Meyer, *Oscillating patterns in image processing and nonlinear evolution equations*, American Mathematical Society, Providence, RI, 2001.

[9] L. Rudin, S. Osher, and E. Fatemi, "Nonlinear total variation based noise removal algorithms," *Physica D*, vol. 60, pp. 259–268, 1992.

[10] W. C. Skamarock, J. B. Klemp, J. Dudhia, D. O. Gill, D. Barker, M. G. Duda, X. Huang, W. Wang, and J. G. Powers, "A description of the advanced research WRF version 3," *University Corporation for Atmospheric Research*, vol. No. NCAR/TN-475+STR, 2008.

[11] Derek J. Posselt, Longtao Wu, Mathias Schreier, Jacola Roman, Masashi Minamide, and Bjorn Lambrigtsen, "Assessing the forecast impact of a geostationary microwave sounder using regional and global OSSEs," *Monthly Weather Review*, vol. 150, no. 3, pp. 625–645, Mar. 2022.